

Characterization of picosecond-scale response time of superconducting NbN hot electron bolometric mixers

Guoao Xie(谢国傲), Ruixuan Tang(唐睿轩), Zhengheng Luo(罗政恒), Jiameng Wang(王家萌), Kangmin Zhou(周康敏), Wei Miao(缪巍), Wen Zhang(张文), Yuan Ren(任远), and Shengcai Shi(史生才)

Citation: Chin. Phys. B, 2026, 35 (**6**): 060601. DOI: 10.1088/1674-1056/ae067a
http://cpb.iphy.ac.cn; http://iopscience.iop.org/cpb

What follows is a list of articles you may be interested in

A real-time performance improvement method for composite time scale

Fangmin Wang(王芳敏), Wenlin Li(李汶林), Hongfei Dai(戴鸿飞), Chunyi Li(李春怡), Jianhua Zhou(周建华), Shenhui Xue(薛申辉), and Bo Wang(王波)

Chin. Phys. B, 2024, 33 (**9**): 090601. DOI: 10.1088/1674-1056/ad6131

Proposal for a realtime Einstein-synchronization-defined satellite virtual clock

Chenhao Yan(严晨皓), Xueyi Tang(汤雪逸), Shiguang Wang(王时光), Lijiaoyue Meng(孟李皎悦), Haiyuan Sun(孙海媛), Yibin He(何奕彬), and Lijun Wang(王力军)

Chin. Phys. B, 2024, 33 (**7**): 070601. DOI: 10.1088/1674-1056/ad3dc9

Robust free-space optical frequency transfer in time-varying link distances conditions

Zhou Tong(童周), Lei Liu(刘雷), Jia-Liang Wang(王家亮), Qian Cao(操前), Zhi-Cheng Jin(金志成), Kang Ying(应康), Shen-Sheng Han(韩申生), Zheng-Fu Han(韩正甫), and You-Zhen Gui(桂有珍)

Chin. Phys. B, 2024, 33 (**2**): 020601. DOI: 10.1088/1674-1056/ad0718

Measurements of Majorana transition frequency shift in caesium atomic fountain clocks

Jun-Ru Shi(施俊如), Xin-Liang Wang(王心亮), Fan Yang(杨帆), Yang Bai(白杨), Yong Guan(管勇), Si-Chen Fan(范思晨), Dan-Dan Liu(刘丹丹), Jun Ruan(阮军), and Shou-Gang Zhang(张首刚)

Chin. Phys. B, 2023, 32 (**4**): 040602. DOI: 10.1088/1674-1056/ac8344

Optical state selection process with optical pumping in a cesium atomic fountain clock

Lei Han(韩蕾), Fang Fang(房芳), Wei-Liang Chen(陈伟亮), Kun Liu(刘昆), Ya-Ni Zuo(左娅妮), Fa-Song Zheng(郑发松), Shao-Yang Dai(戴少阳), and Tian-Chu Li(李天初)

Chin. Phys. B, 2021, 30 (**8**): 080602. DOI: 10.1088/1674-1056/ac0698

Characterization of picosecond-scale response time of superconducting NbN hot electron bolometric mixers

Guoao Xie(谢国傲)[1,2,†], Ruixuan Tang(唐睿轩)[1,2], Zhengheng Luo(罗政恒)[1,2], Jiameng Wang(王家萌)[1,2], Kangmin Zhou(周康敏)[1], Wei Miao(缪巍)[1], Wen Zhang(张文)[1], Yuan Ren(任远)[1,‡], and Shengcai Shi(史生才)[1]

[1] *Purple Mountain Observatory, Chinese Academy of Sciences, Nanjing* 210023, *China*
[2] *University of Science and Technology of China, Hefei* 230026, *China*

(Received 27 June 2025; revised manuscript received 26 August 2025; accepted manuscript online 15 September 2025)

A superconducting hot electron bolometer (HEB) mixer is an ultra-sensitive detector widely used for heterodyne detection of electromagnetic radiation, particularly at terahertz (THz) and submillimeter wavelengths. The response time of an HEB mixer is a critical parameter that defines its dynamic properties. In this work, we employ a pump–probe optical technique to investigate how the response time varies with temperature and bias voltage. Our measurements, conducted at 7 K under bias voltages of 1 mV and 2 mV, reveal a response time of approximately 40 ps. The pump–probe method was introduced to measure the HEB response time for the first time, overcoming conventional electronic bandwidth limitations and achieving picosecond-scale temporal resolution to characterize its ultrafast dynamics in the time domain. Additionally, the results not only reflect the intermediate-frequency noise bandwidth performance of the device but also provide direct guidance for material and fabrication process verification.

Keywords: properties of superconductors, thermodynamic properties, thermoelectric effects, time and frequency

PACS: 06.30.Ft, 74.25.–q, 74.25.Bt, 74.25.fg

DOI: 10.1088/1674-1056/ae067a **CSTR:** 32038.14.CPB.ae067a

1. Introduction

The terahertz (THz) band is typically defined as the frequency range from 0.1 THz to 10 THz, which spans part of the millimeter-wave region, the full submillimeter-wave band, and extends into the lower end of the far-infrared spectrum. It offers promising capabilities for spectroscopy, imaging, and high-resolution sensing.[1] The THz band plays a vital role in astronomical observations, including the study of star and planet formation, the detection of interstellar molecular spectra, and the study of interstellar chemistry.[2] The exceptional sensitivity of superconducting hot-electron bolometer (HEB) mixers makes them widely used in terahertz high-resolution spectroscopy observations, especially at frequencies above 1 THz. The bolometer was first invented by American astronomer Samuel P. Langley in 1881 and was initially applied to study the infrared spectral lines of the Sun. Superconducting HEB mixers operate based on the nonlinear behavior in terms of electron heating and the temperature-dependent resistance around the critical temperature.[3] Since the 1970s, InSb semiconductor HEB mixers have been widely employed due to their relatively high sensitivity.[4] With the advancement of materials science, the superconducting material niobium nitride (NbN), which possesses a relatively high critical temperature (T_c) in the range of 10 K–16 K, has been widely adopted in modern cryogenic applications. Its ultrashort electron–phonon relaxation time — typically on the order of picoseconds — makes it highly suitable for fast response applications, including the heterodyne detection of THz radiation.[5] Instruments such as HIFI on the Herschel Space Telescope,[6] GREAT onboard the SOFIA[7] telescope, and the multibeam receivers on the GUSTO telescope[8] have adopted superconducting NbN HEB mixers as the option for heterodyne detection at THz frequencies. As demonstrated, superconducting NbN is capable of achieving low noise temperature and a broad intermediate frequency bandwidth, making it ideal for high-resolution spectroscopy in the range of 1 THz–5 THz.

Among various HEB types, phonon-cooled HEB has emerged as the dominant architecture due to its large bandwidth and low noise characteristics.[9–11] The phonon-cooling process of an HEB refers to the mechanism by which absorbed electromagnetic energy is transferred from the electron subsystem to the phonon subsystem and subsequently dissipated into the substrate. The operation of such a device is governed by three primary processes: electron–electron scattering, electron–phonon scattering, and phonon escape. A thorough understanding of the thermal transport mechanism in HEB enables the enhancement of bandwidth, thereby improving the overall observational efficiency. Meanwhile, the broadband local oscillator source provided by quantum cas-

[†]Corresponding author. E-mail: xiega@pmo.ac.cn
[‡]Corresponding author. E-mail: yren@pmo.ac.cn

© 2026 Chinese Physical Society and IOP Publishing Ltd. All rights, including for text and data mining, AI training, and similar technologies, are reserved.

cade laser combs[12–14] can be combined with it, enabling simultaneous multi-line detection and broadband communication at THz frequencies.

The phonon cooling time, electron–phonon interaction time, phonon escape time, and diffusion time of superconducting NbN HEB mixers have been calculated on the picosecond scale as functions of critical temperature.[15] Direct response measurement on the picosecond scale requires high-performance sampling equipment and is often susceptible to significant measurement uncertainties. Due to these technical limitations, an accurate measurement of picosecond-scale response time has not yet been fully achieved.

In this paper, measurement of the picosecond-scale response time of the superconducting NbN HEB mixer was conducted by using the pump–probe technique,[16] effectively overcoming the limitations of conventional measurement approaches and enabling more accurate characterization of ultrafast thermal dynamics.

2. Thermal transport mechanism

Hot electron bolometers are highly sensitive detectors that operate based on the nonequilibrium dynamics of electrons in response to incident electromagnetic radiation. Upon absorbing electromagnetic radiation, energy is rapidly transferred to the electron subsystem, leading to an increase in electron temperature while the lattice (phonon system) remains comparatively cool. This creates a transient nonequilibrium state in which the electron and phonon systems maintain distinct temperatures.

This relaxation behavior can be effectively described by a two-temperature model, in which the electron and phonon subsystems are each assigned their own temperature and are thermally coupled:

$$-\frac{\mathrm{d}}{\mathrm{d}x}\left(\lambda_{\mathrm{e}}\frac{\mathrm{d}T_{\mathrm{e}}}{\mathrm{d}x}\right)+C_{\mathrm{e}}\frac{\mathrm{d}T_{\mathrm{e}}}{\mathrm{d}t}+P_{\mathrm{e-p}}=P_{\mathrm{heating}}+P_{\mathrm{p-e}}, \quad (1)$$

$$-\frac{\mathrm{d}}{\mathrm{d}x}\left(\lambda_{\mathrm{p}}\frac{\mathrm{d}T_{\mathrm{p}}}{\mathrm{d}x}\right)+C_{\mathrm{p}}\frac{\mathrm{d}T_{\mathrm{p}}}{\mathrm{d}t}+P_{\mathrm{p-e}}+P_{\mathrm{p-s}}=P_{\mathrm{e-p}}. \quad (2)$$

Here, T_{e} and T_{p} represent the temperatures of the electron and phonon subsystems, respectively. P_{heating} is the total heating power. x is the length of the device, and $\mathrm{d}x$ is the length of a segment. $P_{\mathrm{e-p}}$ denotes the thermal power transferred from the electrons to the phonons, while $P_{\mathrm{p-e}}$ represents the reverse heat flow from the phonons back to the electrons. $P_{\mathrm{p-s}}$ refers to the thermal power conducted from the phonon system to the substrate. C_{e} and C_{p} are the heat capacities, and λ_{e} and λ_{p} are the thermal conductivities of the electron and phonon subsystems, respectively. In the steady state, the temperatures of both the electrons and phonons remain constant over time.

A phonon-cooled superconducting NbN HEB mixer is investigated in this study. The electron–electron scattering time has been experimentally estimated to be on the order of 2 ps at cryogenic temperatures.[17] The electron–phonon scattering time $\tau_{\mathrm{eph}} = 500T_{\mathrm{e}}^{-1.6}$ ps$\cdot$K$^{1.6}$ is typically 1 ps–10 ps, depending on temperature and disorder level.[18] The phonon escape time is $\tau_{\mathrm{esc}} = 10.9$ d$\cdot$ps$\cdot$nm^{-1}.[19] For the phonon-cooled NbN HEB mixer, the response of the HEB is governed by a phonon-cooling process. Therefore, the response time of the NbN HEB mixer is characterized by the phonon cooling time, which is defined as $\tau_{\mathrm{ph}} = \tau_{\mathrm{eph}} + (C_{\mathrm{e}}/C_{\mathrm{p}}) \times \tau_{\mathrm{esc}}$,[9] where the electron heat capacity is $C_{\mathrm{e}} = 1.85 \times 10^{-4} T_{\mathrm{e}}$ J$\cdot$cm$^{-3}\cdot$K^{-2},[18] and the phonon heat capacity is $C_{\mathrm{ph}} = 9.7 \times 10^{-6} T_{\mathrm{e}}^{3}$ J$\cdot$cm$^{-3}\cdot$K^{-4}.[20] Therefore, the response time of the NbN HEB mixer is primarily influenced by T_{e}.

3. Response time measurement

To measure the intrinsic picosecond-scale response time of the superconducting NbN HEB mixer, a pump–probe technique is employed. This method involves varying the delay between two pump pulses while recording the corresponding detector response. By analyzing the change in response as a function of delay time, the behavior of the device can be resolved with picosecond resolution. The experimental setup used for this measurement is illustrated in Fig. 1.

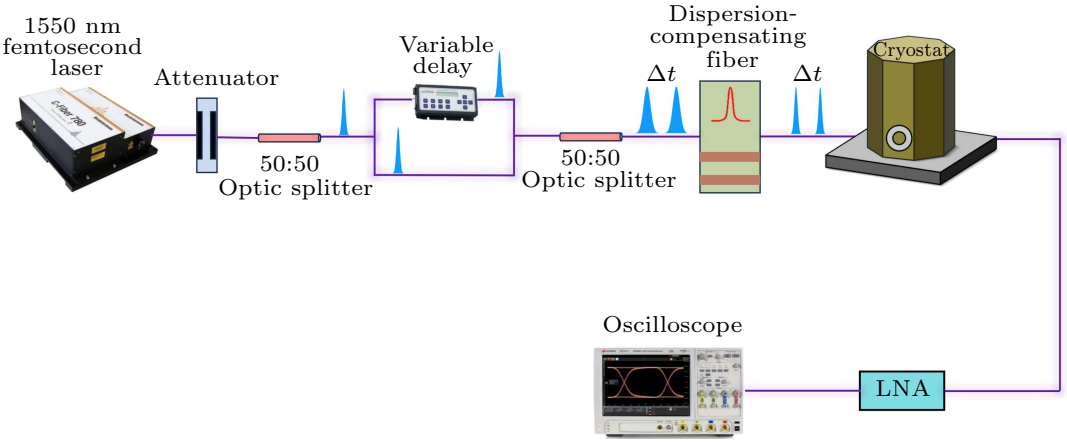


Fig. 1. Schematic diagram of the experimental setup for measuring the picosecond-scale response time of a superconducting NbN HEB mixer using the pump–probe technique.

A femtosecond erbium laser (MenloSystems C-Fiber 780) was utilized as the excitation source, delivering 100-fs pulses at a central wavelength of 1550 nm with a repetition rate of 100 MHz. To avoid saturation of the HEB device and prevent IF amplitude variations arising from nonlinear heating, the laser pulses were attenuated using a tunable fiber attenuator (0–30 dB). The beam was then split into two paths by a 50:50 fused fiber-optic splitter. One path was directed through a miniature motorized variable optical delay line (General Photonics MDL-002) to introduce a controlled delay relative to the other path. Subsequently, the two paths were recombined and coupled into a dispersion-compensating fiber (DCF) to counteract pulse broadening due to dispersion.

Since the refractive index of the fiber material varies with wavelength, the propagation velocity of light becomes wavelength-dependent, which induces dispersion in the fiber. This dispersion broadens the pulse width from the femtosecond scale to 11 ps at the NbN HEB, and DCF was introduced to compensate for the effect. Figure 2(a) shows the pulse widths obtained with different DCF lengths. After incorporating the DCF, the pulse width was effectively reduced to 2 ps. Based on this, a 3.3-meter long DCF was selected, corresponding to the configuration that yielded the minimum achievable pulse width of 2 ps. Although DCF was introduced, the theoretically compressed pulse width is still slightly larger than the original pulse width. As a result, the response time measured with fiber coupling is slightly slower than that obtained using a free-space quasi-optical coupling without dispersion. After compression, the pulse width is approximately 2 ps, comparable to the temporal resolution, so its effect can be considered negligible. For higher temporal resolution, a free-space quasi-optical coupling approach is still required.

Since the pulses emitted by the femtosecond laser were transmitted through an optical fiber, the optical fiber was fixed onto a custom-designed block and aligned using an infrared NIKON MA100 inverted microscope to ensure that the pulses fully illuminated the NbN microbridge. As shown in Fig. 2(b), the center position represents the microbridge, and the optical spot completely covered it. Afterwards, the two delayed pulses were coupled into the fiber and coupled onto the HEB mixer mounted at the 4-K plate of the cryostat. The HEB device is composed of an NbN bridge with dimensions of 1.7 μm in width, 165 nm in length, and 4 nm in thickness, fabricated on a high-resistivity Si substrate. The IF output signal from the HEB mixer corresponded to the illumination from the pulses. These IF signals were initially amplified by a low-noise amplifier operating within the range of 1 GHz–14 GHz at 4 K, followed by further amplification using a room-temperature amplifier covering the range of 1 GHz–18 GHz. The amplified IF signal was then recorded using an oscilloscope (Keysight DSO90804A) with an 8-GHz bandwidth and a sampling rate of 40 GSa/s.

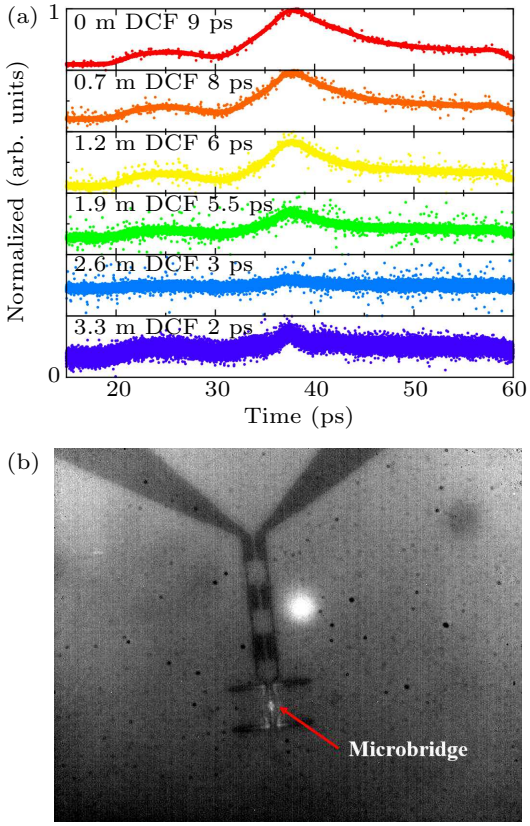


Fig. 2. (a) Dispersion of femtosecond laser pulses after transmission through the single-mode optical fiber in the measurement system, and the resulting pulse width compression achieved by introducing a dispersion-compensating fiber. The pulse width is defined as the full width at half maximum (FWHM) of the pulse. (b) Fiber alignment scan image captured using the infrared NIKON MA100 inverted microscope.

4. Characterization of response time

The HEB response waveforms were sampled with the oscilloscope at a 25-ps time step and subsequently fitted using a Gaussian function with a 0.1-ps time step. The response waveforms at different time delays are shown in Fig. 3(a). Δt is the temporal difference between the two pulses. When the two optical paths are perfectly synchronized, the HEB mixer generates a single-pulse IF response, indicating that both pulses arrive simultaneously and contribute collectively to the response. As the time delay between the two paths is gradually increased, the amplitude of the IF response progressively decreases, while the corresponding pulse width expands. Eventually, when the delay exceeds a certain threshold, the pulses become fully separated, resulting in a distinct dual-pulse excitation response, where each pulse independently contributes to the IF output.

To further analyze this behavior, the response curves of the HEB were measured under varying pulse delays, and the corresponding amplitude values were extracted. This process yielded a variation curve illustrating how the pulse response amplitude changes as a function of time delay. To standardize the analysis and facilitate comparison, the HEB response

was normalized, where the response was set to 1 when the two pulses were completely synchronized, representing the maximum amplitude, and the response was set to 0 when the response amplitude is minimal. Under these defined conditions, the time delay at which the HEB mixer response decreases to the −3 dB of its maximum value is identified as the response time of the superconducting NbN HEB mixer. To accurately determine the pulse overlap point, the time delay was finely adjusted while monitoring the response on the oscilloscope. When the pulses overlap, interference effects occur,[21] leading to fluctuations in the HEB response amplitude. By observing these variations, the overlap point was identified at 32 ps ($\Delta t = 0$ ps). Figures 3(b)–3(e) illustrate the response amplitudes of the superconducting NbN HEB mixer as a function of time delay at various bias voltages (4 mV, 6 mV, 8 mV, and 10 mV) and temperature conditions. The time delay was varied from 0 ps to 400 ps in 2-ps steps. When the time delay reached 32 ps, the two pulses fully overlapped, resulting in a maximum response amplitude. At a time delay of approximately 150 ps, distinct reflections were observed in the curves, attributed to impedance mismatch between the block and the bias tee, leading to signal distortions.

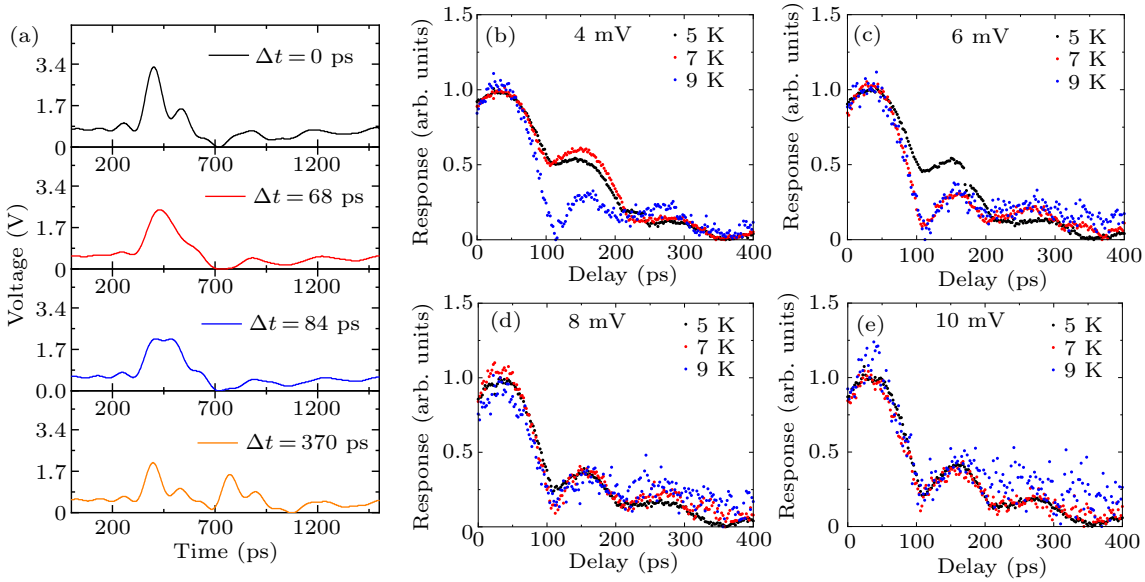


Fig. 3. (a) IF response waveforms of the superconducting NbN HEB mixer at different time delays. As the time delay increases, the response waveform gradually broadens until it eventually splits into two distinct peaks. (b)–(e) Dependence of response amplitude on time delay at different temperatures under bias of 4 mV, 6 mV, 8 mV, and 10 mV.

Higher temperature and bias voltage result in a more pronounced reduction of the response amplitude, indicating a faster response of the HEB mixer. Based on the extracted data, the response times of the superconducting NbN HEB mixer were estimated to be in the range of approximately 50 ps to 80 ps. At a bias voltage of 8 mV, the device operates closer to its normal state, resulting in a reduced response amplitude. This reduction in amplitude, coupled with a degradation in the signal-to-noise ratio, introduces increased uncertainty and error in the response time measurements.

Table 1 summarizes the response times obtained using the pump–probe technique at various temperatures and bias voltages. The results show that the response time decreases with increasing temperature and bias voltage, indicating a faster relaxation process. This trend is consistent with the thermal transport mechanisms in superconducting NbN HEB mixers, where electron–phonon interactions dominate the energy relaxation process. The electron–phonon interaction time exhibits an inverse dependence on temperature, approximately following a $500T_e^{-1.6}$-ps relationship.[18] At temperatures of 5 K, 7 K, and 9 K, the electron–phonon interaction times are approximately 38 ps, 22 ps, and 15 ps, respectively, reflecting the accelerated energy transfer from electrons to phonons at higher temperatures. Enhanced thermal energy at elevated temperatures facilitates faster electron–phonon interactions, improving the overall thermal transport efficiency in the system.

Table 1. Measured response times of superconducting NbN HEB mixer at various bias voltages and temperatures.

Response time (mV)	5 K	7 K	9 K
4	81 ps	74 ps	54 ps
6	72 ps	53 ps	56 ps
8	60 ps	56 ps	52 ps
10	58 ps	50 ps	52 ps

Notably, at high bias and elevated temperatures, the variation in response time becomes minimal and tends to stabilize around 50 ps. As the temperature increases, the response time becomes shorter than the oscilloscope's response time of 54 ps (10%–90%). At this stage, the intrinsic response of the HEB mixer exceeds the temporal resolution of the oscilloscope, resulting in waveform distortion during sampling. This distor-

tion arises because the oscilloscope cannot fully resolve the rapid signal transitions, leading to inaccuracies in the extracted amplitude values of the response time measurement.

5. Temperature correction

To further investigate the relationship between the response time and the IF noise bandwidth, the Y-factor method was employed to measure the IF noise bandwidth of the superconducting NbN HEB mixer. Based on these measurements, the IF noise bandwidth was calculated and compared with the response time obtained from the pump–probe technique. The measured IF noise bandwidth at 3.2 K for the NbN HEB was found to be 5.5 GHz, 4.9 GHz, and 9.9 GHz at 1 mV, 2 mV, and 4 mV, respectively, with the corresponding noise temperatures of 1700 K, 2100 K, and 5000 K. The ratio of the IF noise bandwidth to the IF gain bandwidth in the NbN material is approximately 1.56,[11] yielding a 3-dB IF gain bandwidth of 3.6 GHz. The response time can be expressed as $(2\pi \times \mathrm{IF}_{\mathrm{bandwidth}})^{-1}$,[22] corresponding to a response time of 44 ps. The discrepancy between the IF noise bandwidth corresponding to a response time of 44 ps and the measured response time of 52 ps can be attributed to different HEB states. Since the HEB is in a pumped state during the IF bandwidth measurement, which differs from the HEB unpumped state during the response time measurement with pulsed excitation, the comparison between the IF bandwidth and the response time becomes unreasonable.

To ensure a meaningful comparison between the measured response time and the IF noise bandwidth, the operating temperature of the superconducting HEB mixer was adjusted such that the I–V characteristics in both measurements closely matched. As shown in Fig. 4(a), the I–V curve obtained during the response time measurement at 7.2 K closely resembles the I–V curve obtained in the IF noise bandwidth measurement at 3.2 K. Therefore, the response time measurement at 7.2 K was selected for comparison with the IF noise bandwidth.

Figure 4(b) presents the response time of the superconducting NbN HEB mixer at 7.2 K across different bias voltages using a 26.5-GHz oscilloscope. Exact synchronization of the two pulses was observed at a time delay of 134 ps, while reflections appeared beyond 300 ps. Based on these observations, the intrinsic response time of the superconducting NbN HEB mixer was determined to be approximately 42 ps, which agrees well with the IF gain bandwidth measurement corresponding to a response time of 44 ps. In contrast to IF bandwidths obtained via THz time–domain spectroscopy, the IF bandwidth inferred from the measured response time in this work directly reflects the intrinsic performance of the HEB, rather than the bandwidth corrected with a low-pass filter as reported in Ref. [23]. Furthermore, the measurement obtains the thermal response of the HEB; it is not frequency-selective and does not require the signal source to be matched to the center frequency of the HEB. Therefore, this work provides a direct and reliable approach to link the IF bandwidth with the response time. However, due to the bandwidth limitations of the amplifier employed, it was not possible to accurately resolve response times below 40 ps at higher bias voltages. Notably, the miniature motorized variable optical delay line offers an exceptionally fine delay resolution of 0.3 μm, corresponding to 1 fs, enabling an effective sample rate equivalent to 10^6 GSa/s, which significantly exceeds the capabilities of the oscilloscope. This approach thus provides an effective means of achieving high-resolution measurements.

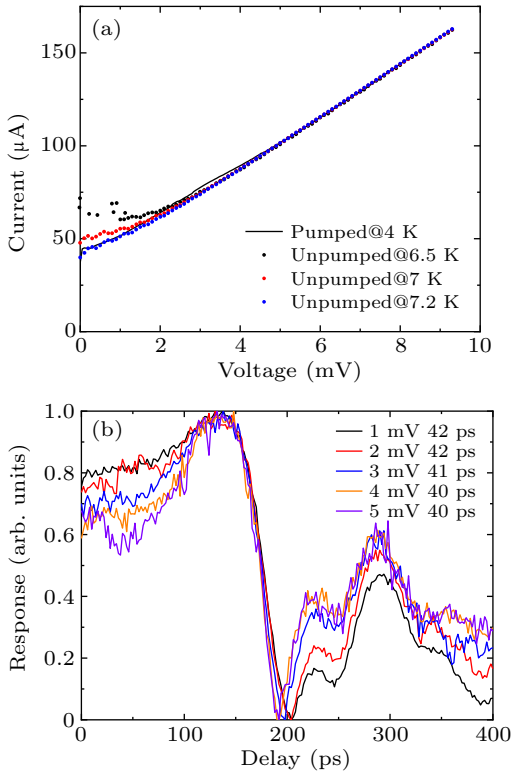


Fig. 4. (a) I–V characteristic curves of the superconducting HEB mixer. The black line represents the pumped I–V curve at 3.2 K during IF noise bandwidth measurement, while the dots correspond to the unpumped I–V curves at 6.5 K (black), 7 K (red), and 7.2 K (blue). (b) Normalized superconducting NbN HEB mixer response amplitudes as a function of time delay at 7.2 K under different bias voltages, measured using a 26.5-GHz oscilloscope.

6. Conclusion

In this study, we investigated the temperature and bias dependence of the superconducting NbN HEB response time by using the pump–probe technique. To address the issues of I–V curve mismatch and the discrepancy between the response time and IF bandwidth, we conducted a pump–probe experiment on the HEB at 7.2 K using a 26.5-GHz oscilloscope. The measured response time was 42 ps, which closely matched the 44 ps derived from the IF noise bandwidth. This method provides valuable insights into the hot electron transport properties of superconducting NbN HEB mixers, which is crucial for optimizing their performance in THz astronomical

observations.

Acknowledgements

Project supported by the Strategic Priority Research Program of the Chinese Academy of Sciences (Grant No. XDB0800000), the National Natural Science Foundation of China (Grant No. 12222308), and the Fund from the Chinese Academy of Sciences (Grant No. PTYQ2024BJ0010).

References

[1] Siegel P 2002 *IEEE Trans Microw Theory Tech.* **50** 910
[2] Phillips T G and Keene J 1992 *Proc. IEEE* **80** 1662
[3] Gershenzon E M, Gol'tsman G N, Gogidze I G, *et al.* 1990 *Sov. Phys. Superconductivity* **3** 1582
[4] Phillips G and Jefferts K B 1973 *Rev. Sci. Instrum.* **44** 1009
[5] Ekstro Èm H and Karasik B 1995 *Appl. Phys. Lett.* **66** 3212
[6] Graauw Th de, Helmich F P, Phillips T G, *et al.* 2010 *A & A* **518** L6
[7] Risacher C, Güsten R, Stutzki J, *et al.* 2018 *A & A* **595** 7
[8] Walker C, Kulesa C, Young A, *et al*. 2022 *The International Society for Opt Engineering* **121900E**
[9] Hajenius M, Baselmans J J A, Gao J R, *et al.* 15*th International Symposium on Space Terahert: Technology* 381
[10] Skalare A, McGrath W R, Bumble B, *et al.* 1996 *Appl. Phys. Lett.* **68** 1558
[11] Ekstroöm H, Kollberg E, Yagoubov P, *et al.* 1997 *Appl. Phys. Lett.* **70** 3296
[12] Li H, Li Z P, Wan W J, *et al.* 2020 *ACS Photon.* **7** 49
[13] Liu G, Ma X, Zhou K, *et al.* 2025 *Light Sci. Appl.* **14** 147
[14] Liu B, Zhou K, Liu G, *et al.* 2025 *Laser Photonics Rev.* **19** 70452
[15] Miao W, Zhang W, Zhou K M, *et al.* 2017 *IEEE Transactions on Applied Superconductivity* **27** 0000201
[16] Carruthers T F and Weller J F 1986 *Appl. Phys. Lett.* **48** 460
[17] Santhanam P and Prober D E 1984 *Phys. Rev. B* **29** 3733
[18] Gousev Yu P, Gol'tsman G, Semenov A D, *et al.* 1994 *Appl. Phys. J.* **75** 3695
[19] Il'in K S, Lindgren M, Currie M, *et al.* 2000 *Appl. Phys. Lett.* **76** 2752
[20] Semenov A D, Nebosis R S, Gousev Y P, *et al.* 1995 *Phys. Rev. B* **52** 581
[21] Marsili F, Stevens M J, Kozorezov A, *et al.* 2016 *Phys. Rev. B* **93** 094518
[22] McGrath W 1995 *Sixth International Symposium on Space Terahertz Technology* 216
[23] Torrioli G, Forrer A, Beck M, *et al.* 2023 *Opt. Express* **31** 15942